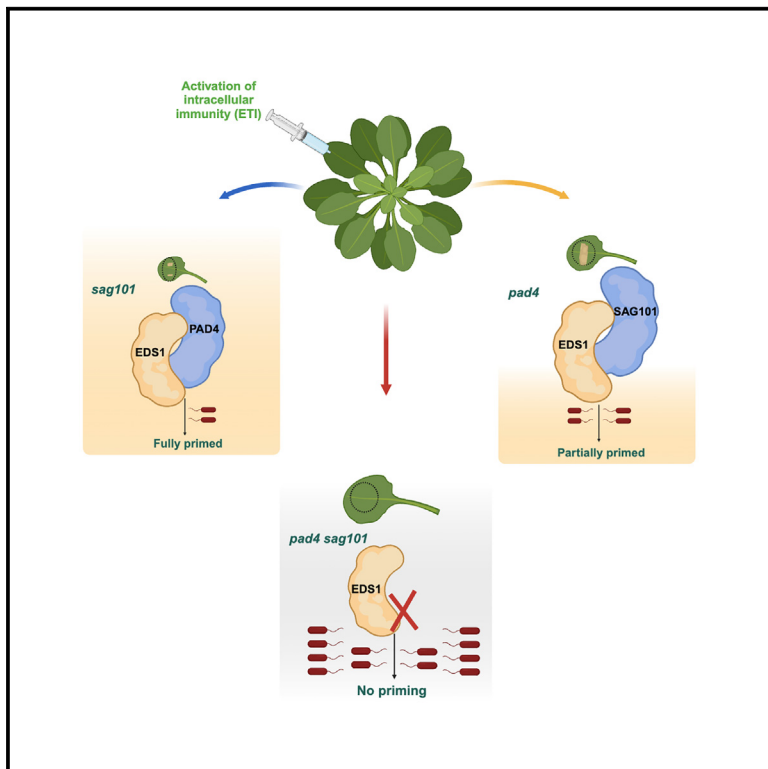


Modular mechanisms of immune priming and growth inhibition mediated by plant effector-triggered immunity

Graphical abstract



Authors

Himanshu Chhillar, Hoang Hung Nguyen, Pei-Min Yeh, Jonathan D.G. Jones, Pingtao Ding

Correspondence

p.ding@biology.leidenuniv.nl

In brief

Chhillar et al. explore effector-triggered immunity (ETI) in plants, highlighting the distinct roles of EDS1 signaling modules. PAD4-ADR1 regulates immune priming and growth inhibition, while SAG101-NRG1 mediates cell death. Their findings offer strategies to enhance crop resistance while minimizing yield loss, advancing sustainable agriculture.

Highlights

- EDS1 signaling modules distinctly regulate ETI in *Arabidopsis*, balancing growth and defense
- PAD4-ADR1 drives immune priming and growth inhibition; SAG101-NRG1 mediates cell death
- Both modules synergize for ETI-induced immune priming, essential for pathogen resistance
- PAD4-ADR1 and SAG101-NRG1 show overlapping but distinct transcriptional responses in ETI



Article

Modular mechanisms of immune priming and growth inhibition mediated by plant effector-triggered immunity

Himanshu Chhillar,¹ Hoang Hung Nguyen,^{1,3} Pei-Min Yeh,^{1,3} Jonathan D.G. Jones,² and Pingtao Ding^{1,4,*}¹Institute of Biology Leiden, Leiden University, Sylviusweg 72, Leiden 2333 BE, the Netherlands²The Sainsbury Laboratory, University of East Anglia, Norwich Research Park, Norwich NR4 7UH, UK³These authors contributed equally⁴Lead contact*Correspondence: p.ding@biology.leidenuniv.nl<https://doi.org/10.1016/j.celrep.2025.115394>**SUMMARY**

Excessive activation of effector-triggered immunity (ETI) in plants inhibits plant growth and activates cell death. ETI mediated by intracellular Toll/interleukin-1 receptor/resistance protein (TIR) nucleotide-binding, leucine-rich repeat receptors (NLRs) involves two partially redundant signaling nodes in *Arabidopsis*, ENHANCED DISEASE SUSCEPTIBILITY 1-PHYTOALEXIN DEFICIENT 4-ACTIVATED DISEASE RESISTANCE 1 (EDS1-PAD4-ADR1) and EDS1-SENESCENCE-ASSOCIATED GENE 101-N REQUIREMENT GENE 1 (EDS1-SAG101-NRG1). Genetic and transcriptomic analyses show that EDS1-PAD4-ADR1 primarily enhances immune component abundance and is critical for limiting pathogen growth, whereas EDS1-SAG101-NRG1 mainly activates the hypersensitive response (HR) cell death but is dispensable for immune priming. This study enhances our understanding of the distinct contributions of these two signaling modules to ETI and suggests molecular principles and potential strategies for improving disease resistance in crops without compromising yield.

INTRODUCTION

Inducible plant defense usually involves the concerted action of responses initiated by cell surface and intracellular immune receptors. Cell surface pattern recognition receptors (PRRs) initiate pattern-triggered immunity (PTI) upon the detection of relatively conserved apoplastic pathogen molecules, such as chitin or flagellin. Effector-triggered immunity (ETI) is activated by intracellular nucleotide-binding, leucine-rich repeat receptors (NLRs) upon recognizing specific pathogen effector proteins.^{1,2} ETI and PTI together confer a highly effective plant defense against pathogen attacks.^{3–5} Recent research has significantly expanded our understanding of the signaling pathways downstream of Toll/interleukin-1 receptor/resistance protein (TIR)-type NLR (TNL)-triggered ETI, with key roles played by lipase-like proteins ENHANCED DISEASE SUSCEPTIBILITY 1 (EDS1), PHYTOALEXIN DEFICIENT 4 (PAD4), and SENESCENCE-ASSOCIATED GENE 101 (SAG101) and helper NLRs ACTIVATED DISEASE RESISTANCE 1 (ADR1) family and N REQUIREMENT GENE 1 (NRG1) family proteins, which share RESISTANCE TO POWDERY MILDEW 8 (RPW8)-like coiled-coil N-terminal signaling domains.^{2,6}

EDS1, PAD4, and SAG101 have emerged as central TNL signaling regulators in *Arabidopsis thaliana* (*Arabidopsis* hereafter) and many other plant species.⁷ These proteins form distinct heterodimeric complexes regulating cell death and dis-

ease resistance.⁸ EDS1-PAD4 complexes have been shown to play a crucial role in local and systemic acquired resistance (SAR).⁹ Meanwhile, EDS1-SAG101 complexes are hypothesized to be more critical for local immune responses, such as constraining the spread of plant viruses.¹⁰ PAD4 and SAG101 also influence salicylic acid (SA) accumulation, connecting hormonal signaling pathways with the regulation of cell death and disease resistance.¹¹

The ADR1 family proteins (ADR1s) in *Arabidopsis* include ADR1, ADR1-LIKE 1 (ADR-L1), and ADR1-L2, which are also known as helper NLR proteins (hNLRs). They are pivotal in controlling ETI.¹² These proteins act as signal amplifiers, promoting the activation of downstream immune responses upon effector recognition.^{2,13} NRG1 hNLR family proteins (NRG1s), including NRG1A (or NRG1.1) and NRG1B (or NRG1.2), are required by TIR-NLRs to drive the hypersensitive response (HR) cell death and contribute to enhanced disease resistance against oomycete pathogens.¹⁴ More recently, it has been shown that the *pad4* mutant mimics *adr1s*, while the *sag101* mutant mimics *nrg1s* in classical immune responses.^{15–17} These genetic results align with the model proposed by several groups that EDS1-PAD4 functions together with ADR1s and contributes more to restricting bacterial growth in TNL-mediated ETI, while EDS1-SAG101 functions with NRG1 and contributes more toward TNL-mediated cell death induced by ETI.^{15–20} These results indicate two distinct



immune regulatory nodes associated with EDS1, leading to different downstream signaling.

The growth-defense trade-off, where plants slow growth in response to pests, is a key principle in plant economics affecting both ecosystems and crop breeding.²¹ Many constitutive ETI mutants with auto-active NLR have shown severe growth penalties,²² which might act via various hormonal signaling pathways while enabling plants to thwart pathogen attacks.²³ Recently, it has been shown that constitutive induction of ETI in the absence of PTI can also effectively lead to significant growth arrest.²⁴ Additionally, prior exposure of plants to pathogens or pathogen-derived ligands primes the plants to induce a much more robust immune response to subsequent encounters.²⁵ For instance, multiple pathogen-associated molecular patterns (PAMPs) have already been shown to prime *Arabidopsis* plants against virulent *Pseudomonas syringae* pv. *tomato* (*Pst*) DC3000 bacterium.²⁶ ETI-induced priming has recently shown a similar effect.²⁴ However, the contribution of crucial immune regulators in governing the phenomenon of ETI-mediated growth-defense trade-off and immune priming remains inadequately understood.

In this study, we unravel the modular signaling pathways downstream of TNL-induced ETI mediated by EDS1-PAD4-ADR1s and EDS1-SAG101-NRG1s, with particular emphasis on their roles in cell death, immune priming, and ETI-induced growth arrest. We have also explored differential transcriptional outcomes between EDS1-PAD4 and EDS1-SAG101 nodes. This work advances our understanding of plant immunity and sheds light on potential strategies for improving disease resistance in crops without impinging on growth and yield.

RESULTS

Differential roles of EDS1-PAD4-ADR1s and EDS1-SAG101-NRG1s in ETI-induced growth arrest

All previous immune phenotypes reported for lipase-like/hNLR mutants were observed during ETI activation in the presence of PTI. Therefore, it was unknown to what extent prior results are ETI specific. Here, we used a β -estradiol (E2)-inducible AvrRps4-expressing (“SETI”) line to activate TNL-mediated ETI in the absence of PTI via the two paired TIR-NLRs RPS4 and RRS1 and RPS4B and RRS1B.²⁴ When growing SETI plants on an E2-containing medium, we observed growth arrest, including a reduction in size and fresh weight (Figures 1A–1C). This growth arrest was suppressed entirely in the *eds1-2* mutant (SETI_eds1) and the *pad4 sag101* double mutant (SETI_ps), indicating a critical role for EDS1, PAD4, and SAG101 in modulating ETI-induced growth inhibition mediated by TNLs.

However, the *sag101* single mutant (SETI_sag101) exhibited a growth inhibition pattern like SETI_wt (wild type) (Figure 1A), implying that SAG101 does not contribute to ETI-induced growth arrest. Interestingly, the *pad4* single mutant (SETI_pad4) appeared to partially suppress the ETI-induced growth arrest in the absence of PTI despite having similar induction in AvrRps4 expression (Figure S1D), suggesting that PAD4 may play a significant role in mediating ETI-dependent growth arrest independent of SAG101 (Figure 1A). Curiously, a severe inhibition in

lateral root formation was observed in SETI_wt and SETI_sag101, which was partially relieved in SETI_pad4 plants and completely relieved in SETI_eds1 and SETI_ps, suggesting a role for PAD4 in controlling root growth and development (Figure 1B).

In parallel, we observed that the *nrg1a nrg1b* double mutant (SETI_nrg1s) mirrored the SETI_sag101 phenotype (Figures S1A–S1C), implying that the NRG1 family proteins may not contribute to growth arrest in response to ETI. Finally, the *adr1 adr1-1/1 adr1-2* triple mutant (SETI_adr1s) resembled the SETI_pad4 phenotype, suggesting a functional correlation between PAD4 and ADR1 proteins in the regulation of ETI-mediated growth arrest.

Distinct contributions to ETI-mediated cell death by PAD4-ADR1s and SAG101-NRG1s

SETI_wt shows no macro cell death induced by ETI in the absence of PTI.²⁴ This hypersensitive response (HR) can be measured by recording ion leakage upon E2 induction, which is easily distinguishable at 4 h post inoculation (hpi) from the mock treatment and saturates at 22 hpi (Figures 2A, S2B, and S3D). SETI_eds1 and SETI_ps plants do not show any significant increase in ionic conductivity upon E2 treatment, highlighting the interplay of EDS1, PAD4, and SAG101 in mediating ETI-mediated cell death.

Interestingly, the increase in ion conductivity in SETI_pad4 upon E2 induction is similar to SETI_wt, suggesting that PAD4 alone is not sufficient to activate ETI-induced cell death (Figure 2A). However, the increase in ion conductivity upon E2 treatment is significantly compromised in SETI_sag101 plants, showing an independent role of SAG101 from PAD4 in mediating ETI-induced cell death in the absence of PTI (Figure 2A). Furthermore, only the SETI_ps mutant can fully compromise ETI-induced ion leakage like SETI_eds1 (Figure 2A). This suggests a synergistic contribution of PAD4 and SAG101 to cell death, as we only see complete abolishment in ion leakage when both PAD4 and SAG101 are lost. We have also observed similar trends in the hNLR mutants in the SETI background (SETI_nrg1s and SETI_adr1s) (Figures S3A and S3D). SETI_adr1s mimics SETI_pad4, while SETI_nrg1s mimics SETI_sag101, showing that the SAG101-NRG1 node might contribute more to ETI-induced cell death, while the PAD4-ADR1 node merely acts as a synergistic module in the presence of the parallel SAG101-NRG1 node.

HR has been shown to have a close association with chlorophyll catabolism.^{27,28} Therefore, we sought to test the chlorophyll content as an additional indicator of cell death. A reduction in total chlorophyll content was observed for SETI_wt and SETI_pad4 upon E2 treatment (Figures 2B and S2A), which was intensified significantly upon the “PTI+ETI” (PTI plus ETI) treatment (50 μ M of E2 and *Pst* DC3000 *hrcC*⁻), which is in line with a previous report.⁴ However, in SETI_sag101, a significant reduction of the total chlorophyll content is observed after PTI+ETI treatment but not after PTI or ETI alone (Figure 2B). This reduction is not as significant as in SETI_pad4 and SETI_wt (Figure 2B). As expected, there is no reduction in chlorophyll content in SETI_ps lines. SETI_adr1s also showed a significant reduction in chlorophyll content upon ETI and PTI+ETI treatments (Figures S3B and S3C), and this reduction is compromised in

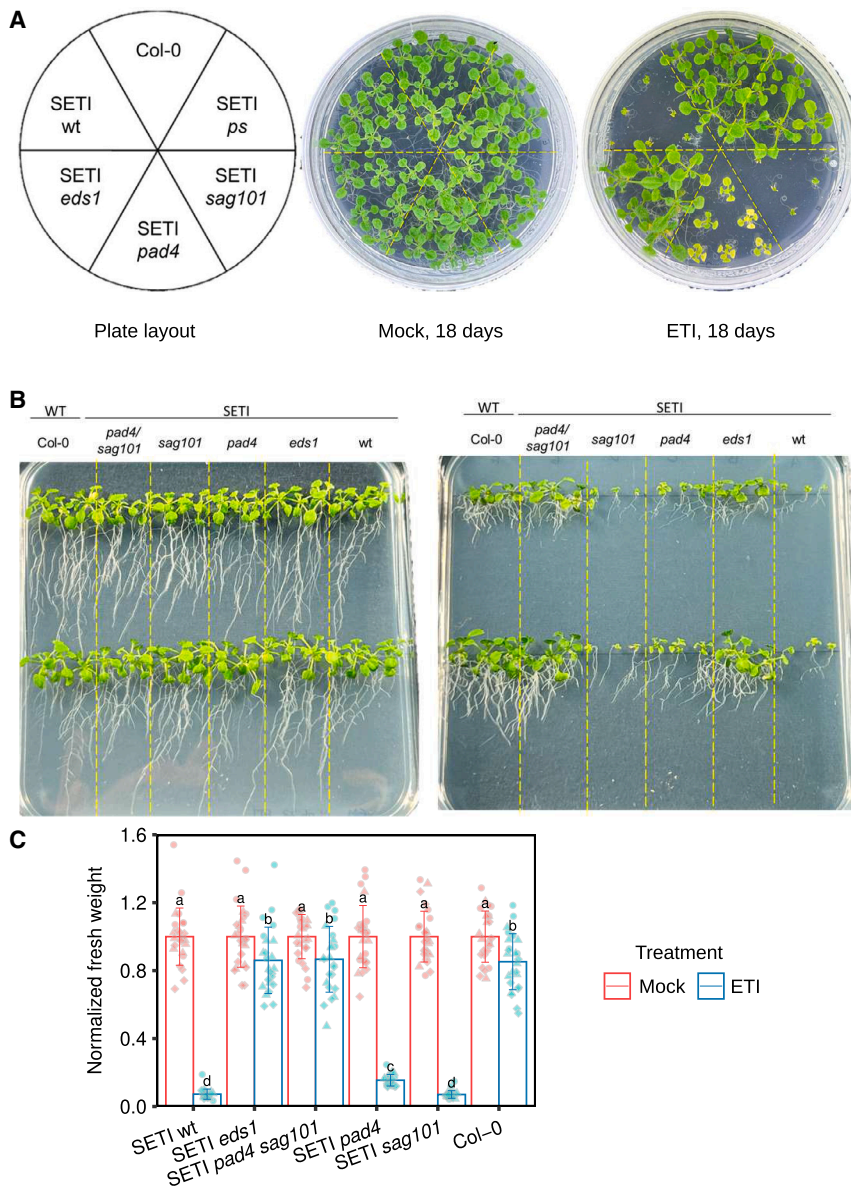


Figure 1. Estradiol-induced growth arrest phenotype in lipase-like protein mutants

(A) Indicated mutants of lipase-like proteins (SETI_wt, SETI_sag101, SETI_pad4, SETI_pad4sag101, and SETI_eds1) were sown on round germination medium (GM) plates with or without E2 (50 μ M), and their growth arrest phenotype was recorded 18 days after planting on E2 plates. (Note: we have used the full name of all the mutants in all the figures for better visualization.)

(B) Indicated mutants of lipase-like proteins were sown on square GM plates without (left) or with (right) 50 μ M E2, and the plates were grown vertically. Growth arrest and lateral root formation phenotypes were recorded 18 days after sowing on E2 plates.

(C) Indicated mutant lines were sown vertically on square GM plates with or without E2 (50 μ M), and the fresh weight was recorded 18 days after sowing on E2 plates. Fresh weight was normalized to the average fresh weight of the mock controls for the respective lines. The error bars show standard deviation. Letters highlight statistical differences (least significant difference [LSD] test, $p \leq 0.05$).

In parallel, we then performed an E2- or ETI-induced disease priming assay with SETI_pad4 and SETI_sag101 mutant plants. We found that the E2-pretreated SETI_sag101 plants show no significant difference from SETI_wt plants in disease resistance priming (Figure 3). Similarly, such a priming effect is retained in SETI_pad4, though overall bacterial growth in E2-pretreated SETI_pad4 plants is higher than that in SETI_wt and SETI_sag101 plants (Figure 3). It is noteworthy that the pad4 but not sag101 mutant was shown to be partially compromised in PTI-primed disease resistance with the elicitor of a 22-amino-acid epitope from bacterial flagellin and fully compromised in nlp20-induced priming,²⁹ indicating that PAD4 may play a more significant role in both ETI- and PTI-primed disease

resistance than SAG101 in *Arabidopsis*, though both PAD4 and SAG101 are required for the disease priming of TNL-mediated ETI.

ETI-mediated immune priming requires both PAD4-ADR1s and SAG101-NRG1s nodes

Pretreatment of SETI_wt plants with E2 shows increased disease resistance against subsequent bacterial infection, indicating that ETI alone can prime plant immunity.²⁴ Consistent with this previous report, we also observed a significant reduction in bacterial growth compared to mock control when SETI_wt plants were pre-infiltrated with E2 1 day before being inoculated with the virulent bacterial strain, *Pst* DC3000 carrying an empty vector (Figure 3). In contrast, E2-pretreated SETI_eds1 and SETI_ps plants show complete loss of priming.

We further tested ETI-mediated disease priming with SETI_nrg1s and SETI_adr1s mutants and the higher-order SETI_helperless mutant, referring to a quintuple mutant with a loss of function of both adr1s and nrg1s, adr1 adr1-11 adr1-12 nrg1a nrg1b.^{15,17} E2-pretreated SETI_nrg1s shows no significant defects in disease priming, which is similar to SETI_wt and SETI_sag101, whereas SETI_adr1s resembles the phenotype of SETI_pad4 (Figure S4). A complete loss in disease priming is only observed in E2-pretreated SETI_helperless plants, and together with the results from SETI_ps (Figures 3 and S4), it can be inferred that both PAD4-ADR1 and SAG101-NRG1 nodes are required for TNL-activated ETI-mediated immune priming.

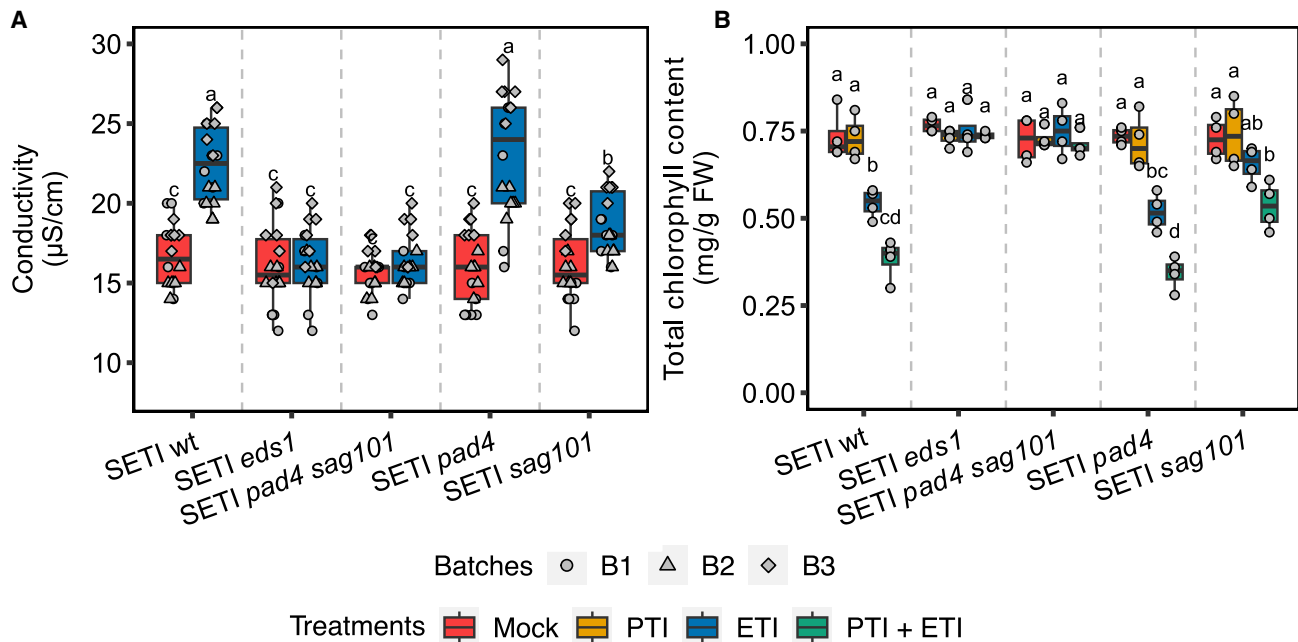


Figure 2. Differential regulation of ETI-induced cell death mediated by lipase-like protein

(A) Indicated mutants of lipase-like proteins (SETI_wt, SETI_sag101, SETI_pad4, SETI_pad4sag101, and SETI_eds1) were infiltrated with E2 or mock, and ion leakage was determined at 24 h time point. Letters show the statistical differences (Tukey honestly significant difference [HSD] test, $p \leq 0.05$).

(B) Total chlorophyll content was estimated on indicated mutants of lipase-like proteins 3 dpi after E2 infiltration as ETI treatment, *Pst* DC3000 *hrcC*⁻ as PTI treatment, (E2 + *Pst* DC3000 *hrcC*⁻) as PTI+ETI treatment, and DMSO dissolved in 10 mM MgCl₂ as mock. Letters represent statistical differences (Tukey HSD test, $p \leq 0.05$).

ETI-specific defense gene profiling mediated by PAD4-ADR1s and SAG101-NRG1s

We performed genome-wide RNA sequencing (RNA-seq) on SETI mutant lines by specifically inducing ETI through E2 treatment to investigate the differences and similarities of defense gene activation between SAG101-NRG1s and PAD4-ADR1s nodes. We found 5,067 differentially expressed genes (DEGs) across all tested genotypes and treatments with $p < 0.01$ and $|\log_2[\text{fold change (FC)}]| \geq 1$ (Figure 4; Tables S1–S11). There are 1,902 up-regulated genes in the SETI_wt, 1,707 up-regulated genes in the SETI_pad4, and 2,281 up-regulated genes in the SETI_sag101 E2-treated samples compared to mock-treated samples (Figure S5B). The DEGs post-E2 treatment, both up-regulated and down-regulated, are substantially reduced in the SETI_pad4 mutant compared to the SETI_wt plants (Figures S5A and S5B), indicating that PAD4 plays a major role in TNL-mediated ETI-induced transcriptional reprogramming and its loss of function could not be compensated by SAG101. Conversely, this reduction in DEG number is not observed in SETI_sag101. Instead, more DEGs are found in SETI_sag101 compared to SETI_wt, which might be due to overcompensation by functional PAD4 or another unknown mechanism of synergy between PAD4 and SAG101. The persistence of DEGs in the SETI_sag101 mutant indicates that SAG101 may not be as critical as PAD4 in suppressing or modulating these gene expressions during ETI early activation. This differential impact on gene expression between the two mutants highlights a divergent role of PAD4 and SAG101 in the plant immune response, emphasizing the complexity of ETI

signaling pathways. These results also highlight the unequal redundancy between PAD4-ADR1s and SAG101-NRG1s, consistent with previous reports that ADR1s can compensate for NRG1s, but not vice versa.¹⁷ There are no DEGs in SETI_eds1 and SETI_pad4 sag101 after E2 treatment compared to mock, demonstrating that the eds1 mutant and pad4 sag101 double mutant can completely block the TNL-mediated ETI-specific transcriptional reprogramming.

Hierarchical clustering of the DEGs in the heatmap revealed 10 clusters using a Euclidean distance and ward.D clustering algorithm (Figure 4).³⁰ Clusters 3, 5, 6, 7, 8, and 9 show defense-related DEGs according to the Gene Ontology (GO) analysis from g:Profiler (false discovery rate [FDR] < 0.05, Benjamini-Hochberg), indicating that these are immune-related clusters (Figure 4). The well-known immune-related genes from each cluster and their expression patterns across the SETI mutants were highlighted (Figure 4; Table S1). Among the immune clusters, cluster 5 comprises genes such as the N-hydroxy piperolic acid (NHP) biosynthetic genes *FMO1* and *ALD1*,³¹ while clusters 5 and 9 contain genes related to cell death. On the other hand, cluster 7 includes genes mainly associated with SA biosynthesis and signaling, like *ICS1*, *EDS5*, and *NPR1*.³² Cluster 8 contains genes related to jasmonate signaling. We further extended our analysis on the downregulated DEGs in clusters 1, 2, 4, and 10, predominantly composed of downregulated genes during ETI early activation. GO term analysis of these clusters revealed that most GO terms are related to hormone response, sugar biosynthesis, sugar metabolism, and

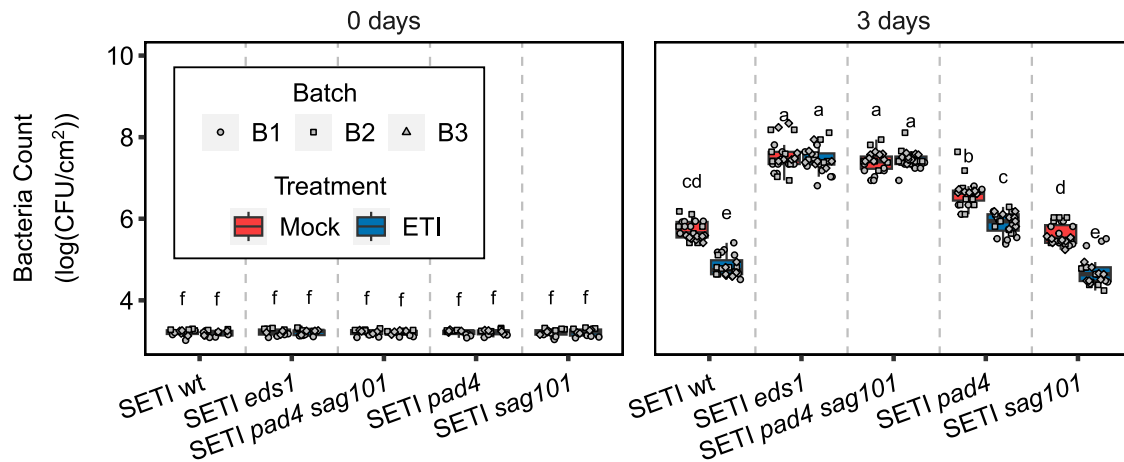


Figure 3. ETI-directed disease priming in SETI lipase-like protein mutants

Indicated mutants of lipase-like proteins were infiltrated with E2 or mock 1 day before infiltration with *Pst* DC3000 carrying the empty vector (EV). Bacterial colony-forming units (CFUs) were counted at days 0 and 3 after infiltration with DC3000 EV. Letters show statistical differences (Tukey HSD test, $p \leq 0.05$).

developmental and photosynthetic pathways (Figures S5C–S5F). This indicates a significant negative influence of ETI activation on specific plant hormonal, cellular, and metabolic processes, aligning with earlier studies.³³ The constitutive effects of this negative influence might be one of the contributing factors to the severe growth retardation of SETI_wt and SETI_sag101 on E2 plates. We also examined the expression profiles of the genes enriched in selected GO terms (Figure S6). Interestingly, the downregulation patterns in SETI_wt and SETI_sag101 are quite similar, whereas SETI_pad4 shows a less pronounced downregulation in a majority of genes related to carbohydrate metabolism, plant morphogenesis, and photosynthesis to some extent (Figure S6). In addition, similar trends were observed concerning hormone pathway genes, including auxin response genes, which play an integral role in lateral root formation.³⁴ These findings provide some initial indications that might explain the partial elevation in growth arrest and lateral root formation observed in SETI_pad4 plants.

Defining the specificity of PAD4- and SAG101-mediated transcriptional reprogramming

The upregulated DEGs were further classified into PAD4- and SAG101-dependent and shared DEGs (Figure 5A; Table S15). A total of 438 DEGs were identified as PAD4 dependent, as they were upregulated in both SETI_wt and SETI_sag101 but downregulated or showed no significant difference in SETI_pad4. Similarly, 85 DEGs were classified as SAG101 dependent, being upregulated in SETI_wt and SETI_pad4 but downregulated or showing no significant difference in SETI_sag101 (Figure 5A). Additionally, 121 DEGs showed shared dependency on both PAD4 and SAG101. Furthermore, 1,258 DEGs were upregulated in SETI_wt, SETI_pad4, and SETI_sag101, indicating that the transcriptional regulation of these DEGs is ETI specific but redundantly regulated by PAD4 and SAG101 (Figures 5A and S7A–S7C). These 1,258 genes were further classified based on partial dependency on PAD4, SAG101, or both (Tables 1 and S16). GO term analysis of these genes

was performed, highlighting those associated with immune-related biological functions (Figures 5B–5D; Tables S12–S14). Interestingly, more DEGs were PAD4 dependent than SAG101 dependent (Figures 5B and 5C). Some genes related to SAR, such as *FMO1* and *ALD1*, were exclusively dependent on PAD4, while other genes showed dependency on both PAD4 and SAG101 (Figures 4, 5B, and 5D; Tables S12 and S14).

It is evident from the ion leakage data that SAG101 contributes more to cell death, but PAD4 has synergistic effects in addition to regulating cell death. As expected, cell-death-related genes were found in all categories, including PAD4 specific, SAG101 specific, and PAD4/SAG101 shared. For instance, genes enriched in cell-death-related GO terms such as *METACASPASE 2 (MC2)*, *MC8*, *CYSTEINE-RICH RECEPTOR-LIKE KINASE 13 (CRK13)*, and *BAX INHIBITOR 1 (BI1)* are found to be dependent on PAD4 (Figure 5B; Table S12). On the other hand, genes like *LAZARUS 5 (LAZ5)* and *CRK4* are dependent on SAG101 (Figure 5C; Table S13), while *BCL-2 ASSOCIATED ATHANOGENE 6 (BAG6)* and *MEMBRANE ATTACK COMPLEX/PERFORIN-LIKE 2 (MACP2)* depend on both PAD4 and SAG101 (Figure 5C; Table S14). Similar observations were made with the downregulated DEGs, with some DEGs being shared and others exclusively regulated by PAD4 or SAG101 (Figure S5A; Table S18).

Collectively, these findings highlight the redundant regulation of transcriptional reprogramming by PAD4 and SAG101, demonstrating that while some DEGs are uniquely controlled by one node, a significant portion are co-regulated by both, underscoring their unequal redundant roles in orchestrating the ETI response. In summary, PAD4 seems to play a prominent role in regulating ETI-activated transcriptional reprogramming compared to SAG101, which may explain why PAD4 contributes more to ETI-induced growth arrest and immune priming, whereas SAG101 plays a more prominent role in cell death. It still needs to be determined how the specificity of transcriptional regulation is achieved by these two unequally redundant nodes downstream of ETI mediated by TNLs.

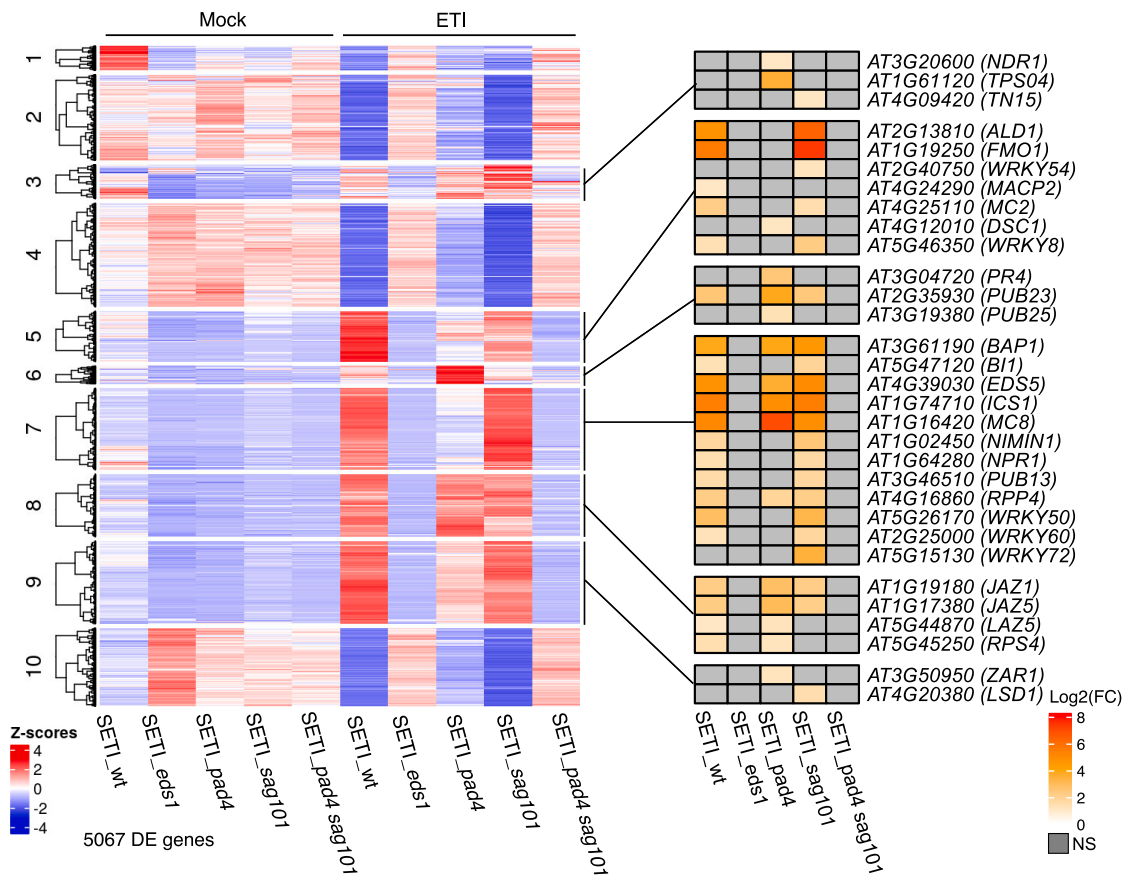


Figure 4. Analysis of TNL-dependent transcriptional changes across SETI lipase-like protein mutants

Five- to six-week-old SETI_wt, SETI_eds1, SETI_pad4, SETI_sag101, and SETI_pad4sag101 plants were infiltrated with mock (10 mM MgCl₂) and 50 μM E2 (ETI). Samples were collected at 4 h post inoculation (4 hpi) for RNA-seq analysis. The left heatmap shows the normalized expression Z score of all the differentially expressed genes with a false discovery rate (FDR) < 0.01 and a log₂fold change of ≥ 1. No significant gene expression changes were seen in SETI_eds1 and SETI_ps after ETI treatment induction. SETI_wt, SETI_pad4, and SETI_sag101 show visible expression after ETI treatment induction. The right heatmap represents the expression pattern of key immune genes upon ETI treatment from each immunity-related cluster among the SETI lipase-like protein mutants, i.e., SETI_wt, SETI_pad4, and SETI_sag101.

DISCUSSION

EDS1 interacts with either of two other lipase-like proteins, PAD4 and SAG101, to initiate the ETI downstream signaling after sensor TNL activation.^{8,35,36} Upon TNL activation, a helper NLR, ADR1 or NRG1, interacts with the EDS1-PAD4 and EDS1-SAG101 modules, respectively.¹⁶ ETI promotes interaction between NRG1 and EDS1/SAG101, but NRG1/EDS1/SAG101 oligomerization requires PTI.^{19,37,38} EDS1-PAD4-ADR1s and EDS1-SAG101-NRG1s have been shown to play unequally redundant roles in plant immune responses.^{16,17} EDS1/PAD4/ADR1s contribute more to disease resistance, while EDS1/SAG101/NRG1s contribute more toward cell death. However, the downstream components and the molecular machinery underlying the unequal roles are still poorly understood.

Here, we focused on investigating ETI-specific roles of the PAD4 and SAG101 nodes. We use the mutants of EDS1 family proteins and helper NLRs in an inducible ETI genetic background to determine the involvement of these proteins in mediating ETI-

specific signaling. Partial relief of growth reduction and inhibition in the lateral root was observed in SETI_pad4 compared to SETI_sag101 on E2 plates, indicating that PAD4 plays an important role in coordinating the balance between growth, development, and defense.²³ SAG101 also synergizes with PAD4 in the growth-defense trade-off, as only the SETI_ps double mutant shows no growth inhibition. As the detailed mechanisms of growth-defense trade-off remain unexplored, our report regarding the differential roles of PAD4 and SAG101 in mediating ETI-specific growth inhibition provides additional information to help decipher the underlying molecular mechanisms.

We define immune priming as the strengthening of plant disease resistance after subjecting plants to a priming treatment. Here, we show that SETI_pad4 (similarly SETI_adr1s) and SETI_sag101 (similarly SETI_nrg1s) both show some immune priming upon ETI activation, though both pad4 (or the adr1s triple mutant) and sag101 (or the nrg1s double mutant) plants are more disease susceptible.^{14,16} These results indicate that plants with partially compromised immunity still retain priming

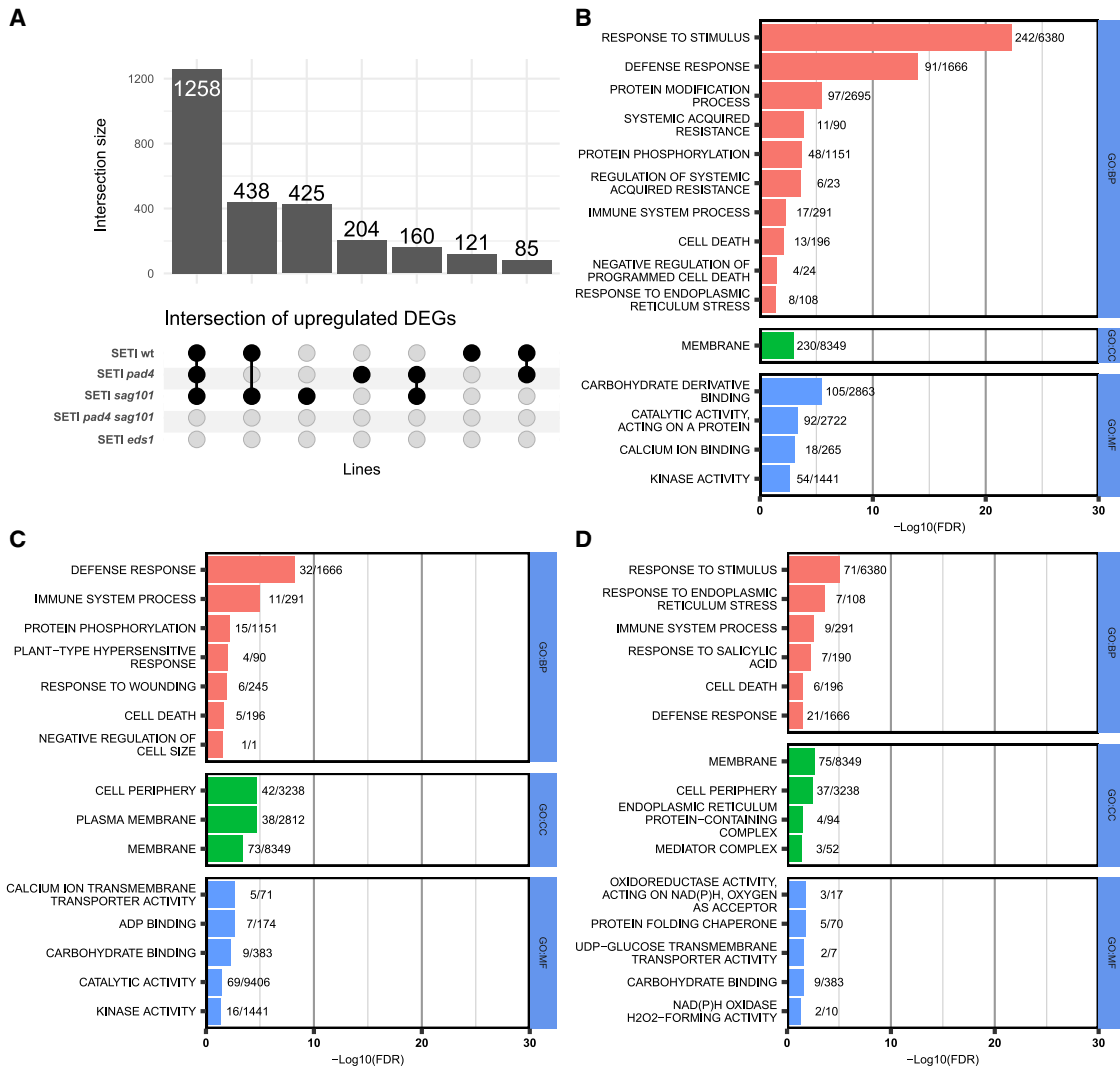


Figure 5. Comparison of gene upregulation in ETI treatments across lipase-like protein mutants

(A) UpSet plot shows 1,258 DEGs affected by both PAD4 and SAG101. 438 DEGs are PAD4 dependent, and 85 DEGs are SAG101 dependent.

(B) GO enrichment for PAD4-dependent DEGs.

(C) GO enrichment for SAG101-dependent DEGs.

(D) GO enrichment for PAD4/SAG101-shared DEGs. GO analysis was done with g:Profiler, and the GO terms are shown in different enrichment analyses, including biological process (GO:BP), cell components (GO:CC), and molecular function (GO:MF) (FDR \leq 0.05, Benjamini-Hochberg).

capacity for disease resistance. This insight could support improved agricultural practices. For instance, for emerging or reemerging pathogens that can partially escape from the immune surveillance system or dampen the immune activation process, one can test whether ETI-mediated immune priming can enhance crop disease resistance. Here, we have only explored the short-term priming capacity in such mutants, and priming could provide longer-term protection. Therefore, it will be interesting to investigate the persistence of this immune memory and how this priming effect has been “memorized” or “imprinted” inside plant cells.

Previous studies have elucidated that HR and disease resistance mechanisms can operate independently.³⁹ Extending

this understanding, our analysis shows that the SAG101-NRG1s module predominantly facilitates ETI-activated cell death, while the PAD4-ADR1s module is more critical for initiating disease resistance. Despite this specificity, both modules have overlapping functions in regulating HR and resistance, though in partially redundant roles. Specifically, NRG1s are required for TNL-mediated disease resistance to obligate biotrophic oomycete pathogens, including the downy mildew agent *Hyaloperonospora arabidopsidis* (*Hpa*) and the white rust causative *Albugo candida*.¹⁴ ADR1s are also required for TNL-mediated resistance against *Hpa*.¹² While the *sag101* single mutant exhibits only isolated single-cell HR cell death, which appears to confer a less severe susceptibility than the *nrg1a nrg1b* double

Table 1. Classification of upregulated genes into partially PAD4-dependent, partially SAG101-dependent, and PAD4/SAG101-dependent categories

Categories	DEG numbers
DEGs partially dependent on <i>PAD4</i> ^a	192
DEGs partially dependent on <i>SAG101</i> ^a	80
DEGs dependent on both <i>PAD4</i> and <i>SAG101</i> ^b	64

^aDEGs present in *SET1_wt*, *SET1_pad4*, and *SET1_sag101*. However, in partially PAD4-dependent DEGs, the log₂ fold change (FC) difference between *SET1* and *SET1_pad4* is greater than 1, but there is no log₂ FC difference between *SET1_wt* and *SET1_sag101*. In partially SAG101-dependent DEGs, the log₂ FC difference between *SET1_wt* and *SET1_sag101* is greater than 1, but there are no difference between *SET1_wt* and *SET1_pad4*.

^bDEGs present in *SET1_wt*, *SET1_pad4*, and *SET1_sag101*. The log₂ FCs between *SET1_wt* and *SET1_pad4* and *SET1_wt* and *SET1_sag101* differ at a magnitude of at least 1.

mutant, both SAG101 and NRG1s are consistently implicated as part of the same downstream signaling pathway mediated by EDS1 in multiple instances.^{14–16,40} The *pad4* single mutant can produce conidiospores accompanied by single-cell trailing necrosis, which aligns with that observed in the *adr1s* triple mutant.^{40,41} More intriguingly, SAG101 and NRG1s appear dispensable for conferring resistance against the hemibiotrophic bacterial pathogen *P. syringae*, where the PAD4-ADR1s node assumes a more important role. Therefore, it is imperative for future studies to comprehensively evaluate disease resistance across a range of mutants, including those carrying mutations in lipase-like protein-encoding genes (*pad4*, *sag101*, and their double mutant), as well as those affecting hNLR-encoding genes (*nrg1s*, *adr1s*, and their quintuple *helperless* mutant). It is also crucial to expand the testing of their responses to include more different types of plant pathogens. Furthermore, it is key to investigate further how each node modulates the functional preference toward HR and resistance and how these are linked to the differential phenotypes of ETI-induced growth inhibition and disease priming. In addition, it will provide valuable insights into NLR-mediated immune effectiveness to explore how the synergistic effects of SAG101-NRG1s and PAD4-ADR1s nodes are achieved.

Importantly, ETI is always preceded by PTI in authentic interactions with microbes, making it challenging to study ETI-specific responses. For instance, in the heatmap that encompasses all the treatments (PTI, ETI, and PTI+ETI), gene expression patterns in PTI+ETI are much less distinguishable across different lipase-like mutants compared to those in the ETI-only treatment (Figure S8). We suspect that PTI can potentially mask the overall ETI transcriptome by pre-emptively activating a set of defense-related pathways that overlap with those induced during ETI. Specifically, PTI-induced genes may saturate the cellular response machinery, thereby attenuating or obscuring the subsequent activation of ETI-specific genes. This is supported by the observation that, in *SET1_wt*, ETI activates a distinct set of genes that are not revealed in combined PTI+ETI treatment via the analysis of DEGs across all conditions (PTI, ETI, and PTI+ETI) (Figure S9; Table S17). This observation reinforces the value of

examining ETI in isolation to identify its unique contributions to gene regulation. In addition, a considerable reduction in the number of upregulated genes in PTI+ETI treatment is observed compared to ETI treatment alone. This suggests that PTI treatment may lead to the expression of specific genes reaching a threshold that renders subsequent responses to ETI less pronounced. This masking effect might explain why the PTI and PTI+ETI profiles appear similar in our heatmap (Figure S8). Moreover, the choice of using the 4 h post inoculation (hpi) time point might have contributed to this observation. This time point is relatively late for capturing early PTI responses⁴² but still within the window where downstream ETI effects could manifest. It is plausible that at this stage, some responses typically associated with ETI could be acting synergistically with PTI, especially since the bacteria utilized have a functional type III secretion system. We also found similar effects in several recent reports.^{17,43} TNLs or TIR-only proteins possess enzymatic activities to produce small molecules that associate with different EDS1 complexes with either PAD4-ADR1s or SAG101-NRG1s.⁴⁴ Our transcriptome profiling results for either PAD4-ADR1s or SAG101-NRG1s modules specific to ETI might provide additional insights. It has been shown that EDS1-SAG101-NRG1s hNLR resistosome formation requires cell surface immune-receptor-mediated PTI; it would be interesting to compare the gene expression patterns between PTI, ETI, and PTI+ETI in *SET1_pad4*. A few other important unresolved questions remain: how do the resistosomes formed by NRG1s and ADR1s activate ETI downstream responses? Are the cation channel activities of NRG1s and ADR1s sufficient to activate the observed transcriptional reprogramming?

More broadly, it has been reported that PAD4 and SAG101 from different plant species may have various functions during TNL-mediated ETI activation. For instance, the Solanaceae genome mainly encodes two SAG101 isoforms (SAG101a and SAG101b), and EDS1-SAG101b has been shown to play a crucial and sufficient role in nearly all TNL-mediated ETI immune responses in *Nicotiana benthamiana* (*Nb*). In contrast, *NbPAD4* did not show any significant roles.³⁶ However, similar to *NbSAG101s*, *NbNRG1* is important in regulating ETI downstream of EDS1 in *Nb*.^{37,45} Conceivably, the EDS1-SAG101-NRG1 node plays a crucial role in regulating both disease resistance and cell death in *Nb*, while in contrast, EDS1-SAG101-NRG1 in *Arabidopsis* is more specialized to HR. It will be interesting in the future to generate ETI-inducible lines in *Nb* that are similar to *SET1* in *Arabidopsis*, to study ETI-specific responses mediated by *NbPAD4* and *NbSAG101* to dissect ETI-specific downstream signaling in comparison to those in *Arabidopsis*, which may provide more insights in ETI-mediated growth-defense trade-off and immune priming. In summary, our studies have provided valuable datasets to dissect modular mechanisms of immune priming and growth inhibition mediated by ETI, which could underpin more innovative plant breeding for disease resistance.

Limitations of the study

Firstly, the study relies on RNA-seq data, which revealed some PAD4- and SAG101-specific components; however, the absence of chromatin immunoprecipitation sequencing (ChIP-seq) and

assay for transposase-accessible chromatin with sequencing (ATAC-seq) datasets precludes the generation of PAD4/SAG101-specific gene regulatory networks (GRNs). The integration of such datasets would provide a more comprehensive understanding of the regulatory mechanisms specific to PAD4 and SAG101. Additionally, our RNA-seq data reflect static gene expression at the peak of early ETI induction and thus fail to capture the temporal dynamics of these regulatory mechanisms, which is a critical aspect for a complete understanding of their role in plant immunity. Secondly, the research focused exclusively on a priming assay tailored for bacterial biotrophs. Whether this response extends to other pathogen categories, such as necrotrophs, remains an important area for future investigation. Thirdly, we acknowledge that the current experimental setup does not allow for distinguishing E2-related effects in WT plants. Consequently, the list of DEGs may also include E2-responsive genes that act independently of the EDS1 family.

RESOURCE AVAILABILITY

Lead contact

Further information and requests for resources and reagents should be directed to and will be fulfilled by the lead contact, Pingtao Ding (p.ding@zenodo.leidenuniv.nl).

Materials availability

Seed generates (see [key resources table](#)) are available upon request from the lead contact.

Data and code availability

- The RNA-seq data for this study have been deposited in the European Nucleotide Archive (ENA) at EMBL-EBI under EMBL-EBI: PRJEB62154.
- All codes are available via GitHub (https://github.com/dinglab-plants/ETI_Project) and deposited in Zenodo under <https://doi.org/10.5281/zenodo.14673399>.
- Any additional information required to reanalyze the data reported in this paper is available from the lead contact upon request.

ACKNOWLEDGMENTS

We thank Marc Gebauer for their technical assistance with the genotyping of mutants and Ewout van Diepen for their invaluable help during the more labor-intensive aspects of our experimentation. Their contributions were instrumental to the successful completion of this work. H.C., H.H.N., P.-M.Y., and P.D. acknowledge European Research Council Starting Grant “R-ELEVATION” (grant agreement: 101039824). J.D.G.J. was supported by the Gatsby Charitable Foundation (UK). We sincerely thank the readers of our initial preprint for their valuable feedback and for pointing out errors. We have incorporated these corrections into this second version. We welcome any further suggestions or comments that can help us improve our manuscript.

AUTHOR CONTRIBUTIONS

P.D. conceptualized and oversaw the inception of the research project. The experimental work was collaboratively conducted by P.D., H.C., and P.-M.Y. Data analysis and figure generation were performed by H.C., H.H.N., P.-M.Y., and P.D. J.D.G.J. was involved throughout the project, providing valuable discussions that significantly shaped the research. H.C. and P.D. wrote the initial manuscript draft. All co-authors contributed to subsequent revisions and editorial processes. The final manuscript was prepared by H.C. and P.D. and was approved for submission by all authors.

DECLARATION OF INTERESTS

The authors declare no competing interests.

STAR★METHODS

Detailed methods are provided in the online version of this paper and include the following:

- [KEY RESOURCES TABLE](#)
- [EXPERIMENTAL MODEL AND STUDY PARTICIPANT DETAILS](#)
 - Plant material and growth conditions
 - Bacterial strains and growth conditions
- [METHOD DETAILS](#)
 - Fresh weight measurement
 - RNA-seq raw data processing, alignment, quantification of expression, and data visualization
 - Electrolyte leakage assay
 - Semi-quantitative real-time PCR
 - Bacterial growth assay
 - Chlorophyll content estimation
- [QUANTIFICATION AND STATISTICAL ANALYSIS](#)

SUPPLEMENTAL INFORMATION

Supplemental information can be found online at <https://doi.org/10.1016/j.celrep.2025.115394>.

Received: February 28, 2024

Revised: December 5, 2024

Accepted: February 13, 2025

REFERENCES

1. Dodds, P.N., and Rathjen, J.P. (2010). Plant immunity: towards an integrated view of plant-pathogen interactions. *Nat. Rev. Genet.* *11*, 539–548. <https://doi.org/10.1038/nrg2812>.
2. Duxbury, Z., Wu, C.-H., and Ding, P. (2021). A comparative overview of the intracellular guardians of plants and animals: nlr in innate immunity and beyond. *Annu. Rev. Plant Biol.* *72*, 155–184. <https://doi.org/10.1146/annurev-arplant-080620-104948>.
3. Jones, J.D.G., and Dangl, J.L. (2006). The plant immune system. *Nature* *444*, 323–329. <https://doi.org/10.1038/nature05286>.
4. Ngou, B.P.M., Ahn, H.-K., Ding, P., and Jones, J.D.G. (2021). Mutual potentiation of plant immunity by cell-surface and intracellular receptors. *Nature* *592*, 110–115. <https://doi.org/10.1038/s41586-021-03315-7>.
5. Yuan, M., Ngou, B.P.M., Ding, P., and Xin, X.-F. (2021). PTI-ETI crosstalk: an integrative view of plant immunity. *Curr. Opin. Plant Biol.* *62*, 102030. <https://doi.org/10.1016/j.pbi.2021.102030>.
6. Parker, J.E., Hessler, G., and Cui, H. (2022). A new biochemistry connecting pathogen detection to induced defense in plants. *New Phytol.* *234*, 819–826. <https://doi.org/10.1111/nph.17924>.
7. Wiermer, M., Feys, B.J., and Parker, J.E. (2005). Plant immunity: the EDS1 regulatory node. *Curr. Opin. Plant Biol.* *8*, 383–389. <https://doi.org/10.1016/j.pbi.2005.05.010>.
8. Wagner, S., Stuttmann, J., Rietz, S., Guerois, R., Brunstein, E., Bautor, J., Niefind, K., and Parker, J.E. (2013). Structural basis for signaling by exclusive EDS1 heteromeric complexes with SAG101 or PAD4 in plant innate immunity. *Cell Host Microbe* *14*, 619–630. <https://doi.org/10.1016/j.chom.2013.11.006>.
9. Bhattacharjee, S., Halane, M.K., Kim, S.H., and Gassmann, W. (2011). Pathogen effectors target Arabidopsis EDS1 and alter its interactions with immune regulators. *Science* *334*, 1405–1408. <https://doi.org/10.1126/science.1211592>.

10. Zhu, S., Jeong, R.-D., Venugopal, S.C., Lapchyk, L., Navarre, D., Kachroo, A., and Kachroo, P. (2011). SAG101 forms a ternary complex with EDS1 and PAD4 and is required for resistance signaling against turnip crinkle virus. *PLoS Pathog.* 7, e1002318. <https://doi.org/10.1371/journal.ppat.1002318>.
11. Vlot, A.C., Dempsey, D.A., and Klessig, D.F. (2009). Salicylic Acid, a multifaceted hormone to combat disease. *Annu. Rev. Phytopathol.* 47, 177–206. <https://doi.org/10.1146/annurev.phyto.050908.135202>.
12. Bonardi, V., Tang, S., Stallmann, A., Roberts, M., Cherkis, K., and Dangl, J.L. (2011). Expanded functions for a family of plant intracellular immune receptors beyond specific recognition of pathogen effectors. *Proc. Natl. Acad. Sci. USA* 108, 16463–16468. <https://doi.org/10.1073/pnas.1113726108>.
13. Dong, O.X., Tong, M., Bonardi, V., El Kasmi, F., Woloshen, V., Wünsch, L.K., Dangl, J.L., and Li, X. (2016). TNL-mediated immunity in Arabidopsis requires complex regulation of the redundant ADR1 gene family. *New Phytol.* 210, 960–973. <https://doi.org/10.1111/nph.13821>.
14. Castel, B., Ngou, P.-M., Cevik, V., Redkar, A., Kim, D.-S., Yang, Y., Ding, P., and Jones, J.D.G. (2019). Diverse NLR immune receptors activate defence via the RPW8-NLR NRG1. *New Phytol.* 222, 966–980. <https://doi.org/10.1111/nph.15659>.
15. Wu, Z., Li, M., Dong, O.X., Xia, S., Liang, W., Bao, Y., Wasteneys, G., and Li, X. (2019). Differential regulation of TNL-mediated immune signaling by redundant helper CNLs. *New Phytol.* 222, 938–953. <https://doi.org/10.1111/nph.15665>.
16. Lapin, D., Kovacova, V., Sun, X., Dongus, J.A., Bhandari, D., von Born, P., Bautor, J., Guarneri, N., Rzemieniewski, J., Stuttmann, J., et al. (2019). A Coevolved EDS1-SAG101-NRG1 Module Mediates Cell Death Signaling by TIR-Domain Immune Receptors. *Plant Cell* 31, 2430–2455. <https://doi.org/10.1105/tpc.19.00118>.
17. Saile, S.C., Jacob, P., Castel, B., Jubic, L.M., Salas-González, I., Bäcker, M., Jones, J.D.G., Dangl, J.L., and El Kasmi, F. (2020). Two unequally redundant “helper” immune receptor families mediate Arabidopsis thaliana intracellular “sensor” immune receptor functions. *PLoS Biol.* 18, e3000783. <https://doi.org/10.1371/journal.pbio.3000783>.
18. Collier, S.M., Hamel, L.-P., and Moffett, P. (2011). Cell death mediated by the N-terminal domains of a unique and highly conserved class of NB-LRR protein. *Mol. Plant Microbe Interact.* 24, 918–931. <https://doi.org/10.1094/MPMI-03-11-0050>.
19. Sun, X., Lapin, D., Feehan, J.M., Stolze, S.C., Kramer, K., Dongus, J.A., Rzemieniewski, J., Blanvillain-Baufumé, S., Harzen, A., Bautor, J., et al. (2021). Pathogen effector recognition-dependent association of NRG1 with EDS1 and SAG101 in TNL receptor immunity. *Nat. Commun.* 12, 3335. <https://doi.org/10.1038/s41467-021-23614-x>.
20. Wu, Z., Tian, L., Liu, X., Zhang, Y., and Li, X. (2021). TIR signal promotes interactions between lipase-like proteins and ADR1-L1 receptor and ADR1-L1 oligomerization. *Plant Physiol.* 187, 681–686. <https://doi.org/10.1093/plphys/kiab305>.
21. He, Z., Webster, S., and He, S.Y. (2022). Growth-defense trade-offs in plants. *Curr. Biol.* 32, R634–R639. <https://doi.org/10.1016/j.cub.2022.04.070>.
22. van Wersch, R., Li, X., and Zhang, Y. (2016). Mighty dwarfs: Arabidopsis autoimmune mutants and their usages in genetic dissection of plant immunity. *Front. Plant Sci.* 7, 1717. <https://doi.org/10.3389/fpls.2016.01717>.
23. Denancé, N., Sánchez-Vallet, A., Goffner, D., and Molina, A. (2013). Disease resistance or growth: the role of plant hormones in balancing immune responses and fitness costs. *Front. Plant Sci.* 4, 155. <https://doi.org/10.3389/fpls.2013.00155>.
24. Ngou, B.P.M., Ahn, H.-K., Ding, P., Redkar, A., Brown, H., Ma, Y., Youles, M., Tomlinson, L., and Jones, J.D.G. (2020). Estradiol-inducible AvrRps4 expression reveals distinct properties of TIR-NLR-mediated effector-triggered immunity. *J. Exp. Bot.* 71, 2186–2197. <https://doi.org/10.1093/jxb/erz571>.
25. Cooper, A., and Ton, J. (2022). Immune priming in plants: from the onset to transgenerational maintenance. *Essays Biochem.* 66, 635–646. <https://doi.org/10.1042/EBC20210082>.
26. Liu, J., Ding, P., Sun, T., Nitta, Y., Dong, O., Huang, X., Yang, W., Li, X., Botella, J.R., and Zhang, Y. (2013). Heterotrimeric G proteins serve as a converging point in plant defense signaling activated by multiple receptor-like kinases. *Plant Physiol.* 161, 2146–2158. <https://doi.org/10.1104/pp.112.212431>.
27. Mur, L.A.J., Aubry, S., Mondhe, M., Kingston-Smith, A., Gallagher, J., Timms-Taravella, E., James, C., Papp, I., Hörtensteiner, S., Thomas, H., and Ougham, H. (2010). Accumulation of chlorophyll catabolites photosensitizes the hypersensitive response elicited by *Pseudomonas syringae* in Arabidopsis. *New Phytol.* 188, 161–174. <https://doi.org/10.1111/j.1469-8137.2010.03377.x>.
28. Mur, L.A.J., Kenton, P., Lloyd, A.J., Ougham, H., and Prats, E. (2008). The hypersensitive response; the centenary is upon us but how much do we know? *J. Exp. Bot.* 59, 501–520. <https://doi.org/10.1093/jxb/erm239>.
29. Pruitt, R.N., Locci, F., Wanke, F., Zhang, L., Saile, S.C., Joe, A., Karelina, D., Hua, C., Fröhlich, K., Wan, W.-L., et al. (2021). The EDS1-PAD4-ADR1 node mediates Arabidopsis pattern-triggered immunity. *Nature* 598, 495–499. <https://doi.org/10.1038/s41586-021-03829-0>.
30. Saraçlı, S., Doğan, N., and Doğan, İ. (2013). Comparison of hierarchical cluster analysis methods by cophenetic correlation. *J. Inequalities Appl.* 2013, 203. <https://doi.org/10.1186/1029-242X-2013-203>.
31. Ding, P., Rekhter, D., Ding, Y., Feussner, K., Busta, L., Haroth, S., Xu, S., Li, X., Jetter, R., Feussner, I., and Zhang, Y. (2016). Characterization of a piperolic acid biosynthesis pathway required for systemic acquired resistance. *Plant Cell* 28, 2603–2615. <https://doi.org/10.1105/tpc.16.00486>.
32. Ding, P., and Ding, Y. (2020). Stories of salicylic acid: A plant defense hormone. *Trends Plant Sci.* 25, 549–565. <https://doi.org/10.1016/j.tplants.2020.01.004>.
33. Rojas, C.M., Senthil-Kumar, M., Tzin, V., and Mysore, K.S. (2014). Regulation of primary plant metabolism during plant-pathogen interactions and its contribution to plant defense. *Front. Plant Sci.* 5, 17. <https://doi.org/10.3389/fpls.2014.00017>.
34. Du, Y., and Scheres, B. (2018). Lateral root formation and the multiple roles of auxin. *J. Exp. Bot.* 69, 155–167. <https://doi.org/10.1093/jxb/erx223>.
35. Rietz, S., Stamm, A., Malonek, S., Wagner, S., Becker, D., Medina-Escobar, N., Corina Vlot, A., Feys, B.J., Niefind, K., and Parker, J.E. (2011). Different roles of Enhanced Disease Susceptibility1 (EDS1) bound to and dissociated from Phytoalexin Deficient4 (PAD4) in Arabidopsis immunity. *New Phytol.* 191, 107–119. <https://doi.org/10.1111/j.1469-8137.2011.03675.x>.
36. Gantner, J., Ordon, J., Kretschmer, C., Guerois, R., and Stuttmann, J. (2019). An EDS1-SAG101 complex is essential for TNL-mediated immunity in *Nicotiana benthamiana*. *Plant Cell* 31, 2456–2474. <https://doi.org/10.1105/tpc.19.00099>.
37. Qi, T., Seong, K., Thomazella, D.P.T., Kim, J.R., Pham, J., Seo, E., Cho, M.-J., Schultink, A., and Staskawicz, B.J. (2018). NRG1 functions downstream of EDS1 to regulate TIR-NLR-mediated plant immunity in *Nicotiana benthamiana*. *Proc. Natl. Acad. Sci. USA* 115, E10979–E10987. <https://doi.org/10.1073/pnas.1814856115>.
38. Feehan, J.M., Wang, J., Sun, X., Choi, J., Ahn, H.-K., Ngou, B.P.M., Parker, J.E., and Jones, J.D.G. (2023). Oligomerization of a plant helper NLR requires cell-surface and intracellular immune receptor activation. *Proc. Natl. Acad. Sci. USA* 120, e2210406120. <https://doi.org/10.1073/pnas.2210406120>.
39. de Ronde, D., Butterbach, P., and Kormelink, R. (2014). Dominant resistance against plant viruses. *Front. Plant Sci.* 5, 307. <https://doi.org/10.3389/fpls.2014.00307>.
40. Feys, B.J., Wiermer, M., Bhat, R.A., Moisan, L.J., Medina-Escobar, N., Neu, C., Cabral, A., and Parker, J.E. (2005). Arabidopsis SENESCENCE-ASSOCIATED GENE101 stabilizes and signals within an ENHANCED

- DISEASE SUSCEPTIBILITY1 complex in plant innate immunity. *Plant Cell* 17, 2601–2613. <https://doi.org/10.1105/tpc.105.033910>.
41. Bonardi, V., Cherkis, K., Nishimura, M.T., and Dangl, J.L. (2012). A new eye on NLR proteins: focused on clarity or diffused by complexity? *Curr. Opin. Immunol.* 24, 41–50. <https://doi.org/10.1016/j.coi.2011.12.006>.
 42. Bjornson, M., Pimprikar, P., Nürnberger, T., and Zipfel, C. (2021). The transcriptional landscape of *Arabidopsis thaliana* pattern-triggered immunity. *Nat. Plants* 7, 579–586. <https://doi.org/10.1038/s41477-021-00874-5>.
 43. Ding, P., Sakai, T., Krishna Shrestha, R., Manosalva Perez, N., Guo, W., Ngou, B.P.M., He, S., Liu, C., Feng, X., Zhang, R., et al. (2021). Chromatin accessibility landscapes activated by cell-surface and intracellular immune receptors. *J. Exp. Bot.* 72, 7927–7941. <https://doi.org/10.1093/jxb/erab373>.
 44. Locci, F., Wang, J., and Parker, J.E. (2023). TIR-domain enzymatic activities at the heart of plant immunity. *Curr. Opin. Plant Biol.* 74, 102373. <https://doi.org/10.1016/j.pbi.2023.102373>.
 45. Peart, J.R., Mestre, P., Lu, R., Malcuit, I., and Baulcombe, D.C. (2005). NRG1, a CC-NB-LRR protein, together with N, a TIR-NB-LRR protein, mediates resistance against tobacco mosaic virus. *Curr. Biol.* 15, 968–973. <https://doi.org/10.1016/j.cub.2005.04.053>.
 46. Thomas, W.J., Thireault, C.A., Kimbrel, J.A., and Chang, J.H. (2009). Recombining and stable integration of the *Pseudomonas syringae* pv. *syringae* 61 hrp/hrc cluster into the genome of the soil bacterium *Pseudomonas fluorescens* Pf0-1. *Plant J.* 60, 919–928. <https://doi.org/10.1111/j.1365-3113X.2009.03998.x>.
 47. Petnicki-Ocwieja, T., van Dijk, K., and Alfano, J.R. (2005). The hrpK operon of *Pseudomonas syringae* pv. *tomato* DC3000 encodes two proteins secreted by the type III (Hrp) protein secretion system: HopB1 and HrpK, a putative type III translocator. *J. Bacteriol.* 187, 649–663. <https://doi.org/10.1128/JB.187.2.649-663.2005>.
 48. Sohn, K.H., Zhang, Y., and Jones, J.D.G. (2009). The *Pseudomonas syringae* effector protein, AvrRPS4, requires in planta processing and the KRVY domain to function. *Plant J.* 57, 1079–1091. <https://doi.org/10.1111/j.1365-3113X.2008.03751.x>.
 49. Wickham, H., Averick, M., Bryan, J., Chang, W., McGowan, L., François, R., Grolemund, G., Hayes, A., Henry, L., Hester, J., et al. (2019). Welcome to the tidyverse. *J. Open Source Softw.* 4, 1686. <https://doi.org/10.21105/joss.01686>.
 50. Gu, Z., Gu, L., Eils, R., Schlesner, M., and Brors, B. (2014). circlize Implements and enhances circular visualization in R. *Bioinformatics* 30, 2811–2812. <https://doi.org/10.1093/bioinformatics/btu393>.
 51. Lex, A., Gehlenborg, N., Strobel, H., Vuilleumot, R., and Pfister, H. (2014). Upset: visualization of intersecting sets. *IEEE Trans. Vis. Comput. Graph.* 20, 1983–1992. <https://doi.org/10.1109/TVCG.2014.2346248>.
 52. Blighe, K., Rana, S., and Lewis, M. (2022). EnhancedVolcano: Publication-ready volcano plots with enhanced colouring and labeling. *Bioconductor* 7, 10–18129. <https://doi.org/10.18129/b9.bioc.enhancedvolcano>.
 53. Iannone, R., Cheng, J., Schloerke, B., Hughes, E., Lauer, A., Seo, J., Brevoort, K., and Roy, O. (2024). gt: Easily Create Presentation-Ready Display Tables <https://gt.rstudio.com/>.
 54. Mock, T. (2023). gtExtras: Extending “gt”. Preprint at bioRxiv. <https://github.com/jthomasmock/gtExtras>.
 55. Wickham, H. (2023). stringr: Simple, Consistent Wrappers for Common String Operations. <https://stringr.tidyverse.org/>
 56. Graves, S., Piepho, H.-P., and Selzer, L. (2023). multcompView: Visualizations of Paired Comparisons. <https://cran.r-project.org/web/packages/multcompView/index.html>
 57. de Mendiburu, F. (2023). agricolae: Statistical Procedures for Agricultural Research. <https://cran.r-project.org/web/packages/agricolae/index.html>
 58. Kassambara, A. ggpubr: ‘ggplot2’ Based Publication Ready Plots. <https://rpkgs.datanovia.com/ggpubr/>.
 59. Gherardi, V. (2021). r2r: R-Object to R-Object Hash Maps. <https://cran.r-project.org/web/packages/r2r/vignettes/r2r.html>
 60. Kolberg, L., Raudvere, U., Kuzmin, I., Adler, P., Vilo, J., and Peterson, H. (2023). g:Profiler-interoperable web service for functional enrichment analysis and gene identifier mapping (2023 update). *Nucleic Acids Res.* 51, W207–W212. <https://doi.org/10.1093/nar/gkad347>.
 61. Guo, W., Tzioutziou, N.A., Stephen, G., Milne, I., Calixto, C.P., Waugh, R., Brown, J.W.S., and Zhang, R. (2021). 3D RNA-seq: a powerful and flexible tool for rapid and accurate differential expression and alternative splicing analysis of RNA-seq data for biologists. *RNA Biol.* 18, 1574–1587. <https://doi.org/10.1080/15476286.2020.1858253>.
 62. Bjornson, M., Kajala, K., Zipfel, C., and Ding, P. (2020). Low-cost and High-throughput RNA-seq Library Preparation for Illumina Sequencing from Plant Tissue. *Bio. Protoc.* 10, e3799. <https://doi.org/10.21769/Bio-Protoc.3799>.
 63. Andrews, S. (2023). FastQC.
 64. Zhang, R., Kuo, R., Coulter, M., Calixto, C.P.G., Entizne, J.C., Guo, W., Marquez, Y., Milne, L., Riegler, S., Matsui, A., et al. (2022). A high-resolution single-molecule sequencing-based *Arabidopsis* transcriptome using novel methods of Iso-seq analysis. *Genome Biol.* 23, 149. <https://doi.org/10.1186/s13059-022-02711-0>.
 65. Bray, N.L., Pimentel, H., Melsted, P., and Pachter, L. (2016). Near-optimal probabilistic RNA-seq quantification. *Nat. Biotechnol.* 34, 525–527. <https://doi.org/10.1038/nbt.3519>.
 66. Risso, D., Ngai, J., Speed, T.P., and Dudoit, S. (2014). Normalization of RNA-seq data using factor analysis of control genes or samples. *Nat. Biotechnol.* 32, 896–902. <https://doi.org/10.1038/nbt.2931>.
 67. Robinson, M.D., and Oshlack, A. (2010). A scaling normalization method for differential expression analysis of RNA-seq data. *Genome Biol.* 11, R25. <https://doi.org/10.1186/gb-2010-11-3-r25>.
 68. Law, C.W., Chen, Y., Shi, W., and Smyth, G.K. (2014). voom: Precision weights unlock linear model analysis tools for RNA-seq read counts. *Genome Biol.* 15, R29. <https://doi.org/10.1186/gb-2014-15-2-r29>.
 69. Ritchie, M.E., Phipson, B., Wu, D., Hu, Y., Law, C.W., Shi, W., and Smyth, G.K. (2015). limma powers differential expression analyses for RNA-sequencing and microarray studies. *Nucleic Acids Res.* 43, e47. <https://doi.org/10.1093/nar/gkv007>.
 70. Chazaux, M., Schiphorst, C., Lazzari, G., and Caffarri, S. (2022). Precise estimation of chlorophyll a, b and carotenoid content by deconvolution of the absorption spectrum and new simultaneous equations for Chl determination. *Plant J.* 109, 1630–1648. <https://doi.org/10.1111/tbj.15643>.
 71. Gu, Z. (2022). Complex heatmap visualization. *iMeta* 1, e43. <https://doi.org/10.1002/imt2.43>.

STAR★METHODS

KEY RESOURCES TABLE

REAGENT or RESOURCE	SOURCE	IDENTIFIER
Bacterial and virus strains		
<i>Pseudomonas fluorescens</i> (Pf0-1)	Thomas et al. ⁴⁶	N/A
<i>Pst</i> DC3000 <i>hrcC</i>	Petnicki-Ocwieja et al. ⁴⁷	N/A
<i>Pst</i> DC3000 EV	Sohn et al. ⁴⁸	N/A
Biological samples		
<i>Arabidopsis thaliana</i> : Col-0 (WT)	Ngou et al. ²⁴	N/A
<i>Arabidopsis thaliana</i> : SET1 (SET1_wt)	Ngou et al. ²⁴	N/A
<i>Arabidopsis thaliana</i> : SET1 <i>eds1-2</i> (SET1_eds1)	This study	N/A
<i>Arabidopsis thaliana</i> : SET1 <i>pad4-1</i> (SET1_pad4)	This study	N/A
<i>Arabidopsis thaliana</i> : SET1 <i>sag101-1</i> (SET1_sag101)	This study	N/A
<i>Arabidopsis thaliana</i> : SET1 <i>pad4-1 sag101-1</i> (SET1_ps)	This study	N/A
<i>Arabidopsis thaliana</i> : SET1 <i>adr1-1 adr1-L1 adr1-L2 nrg1a nrg1b</i> (SET1_helperless)	This study	N/A
<i>Arabidopsis thaliana</i> : SET1 <i>nrg1a nrg1b</i> (SET1_nrg1s)	This study	N/A
<i>Arabidopsis thaliana</i> : SET1 <i>adr1-1 adr1-L1 adr1-L2</i> (SET1_adr1s)	This study	N/A
<i>Arabidopsis thaliana</i> : <i>eds1-2</i>	Feys et al. ⁴⁰	N/A
<i>Arabidopsis thaliana</i> : <i>pad4-1</i>	Feys et al. ⁴⁰	N/A
<i>Arabidopsis thaliana</i> : <i>sag101-1</i>	Feys et al. ⁴⁰	N/A
<i>Arabidopsis thaliana</i> : <i>pad4-1 sag101-1</i>	This study	N/A
<i>Arabidopsis thaliana</i> : <i>adr1-1 adr1-L1 adr1-L2</i>	Bonardi et al. ¹²	N/A
<i>Arabidopsis thaliana</i> : <i>nrg1a nrg1b</i>	Castel et al. ¹⁴	N/A
<i>Arabidopsis thaliana</i> : <i>helperless</i>	Saile et al. ¹⁷	N/A
Chemicals, peptides, and recombinant proteins		
Dimethyl sulfoxide (DMSO)	Sigma	Cat# D8418
β-Estradiol	Sigma	Cat# E8875
Magnesium chloride hexahydrate	MERCK	Ca# M9272
Agarose	VWR	Cat# 732-2789
Murashige & Skoog medium including vitamins	Duchefa	Cat# M0222
Oxoid™ Peptone Bacteriological Neutralized	Thermo Scientific	LP0034B
Critical commercial assays		
HiScript II Reverse Transcriptase	Vazyme	Cat# RL-201-02
DNase I, RNase-free	Vazyme	Cat# EN402-01
RNA Wash Buffer	Zymo Research	Cat# R1003-3-24
RNA Prep Buffer	Zymo Research	Cat# R1060-2-100
Zymo-Spin IICR Columns	Zymo Research	Cat# C1078-250
Murine RNase Inhibitor	Vazyme	Cat# R301-03
Deposited data		
Raw RNA-seq Dataset	This study; NCBI	ENA: PRJEB62154
Source data and statistical summary	This study	Zenodo: https://doi.org/10.5281/zenodo.14673399
Oligonucleotides		
<i>AvrRps4_F</i> : 5'-TCCAGCTTCAGTTACTCGGC-3'	This study	N/A
<i>AvrRps4_R</i> : 5'-TTGGCTATTTCCGGCTGGGTT-3'	This study	N/A

(Continued on next page)

Continued		
REAGENT or RESOURCE	SOURCE	IDENTIFIER
<i>EF1α_F</i> : 5'-CAGGCTGATTGTGCTGTTCTTA-3'	Ngou et al. ²⁴	N/A
<i>EF1α_R</i> : 5'GTTGTATCCGACCTTCTTCAGG-3'	Ngou et al. ²⁴	N/A
Oligo-dT: 5'-TTTTTTTTTTTTTTTTT-3'	N/A	N/A
Software and algorithms		
GGplot2	Wickham ⁴⁹	N/A
ComplexHeatmap	Gu ⁵⁰	N/A
ComplexUpset	Lex et al. ⁵¹	N/A
EnhancedVolcano	Blighe et al. ⁵²	N/A
gt	Iannone et al. ⁵³	N/A
gtExtras	Mock ⁵⁴	N/A
Tidverse	Wickham et al. ⁵⁵	N/A
multcompView	Graves et al. ⁵⁶	N/A
agricolae	de Mendiburu ⁵⁷	N/A
ggpubr	Kassambara ⁵⁸	N/A
stringr	Wickham ⁵⁵	N/A
r2r	Gherardi ⁵⁹	N/A
circlize	Gu et al. ⁵⁰	N/A
g:Profiler	Kolberg et al. ⁶⁰	N/A
3D RNA-seq software	Guo et al. ⁶¹	N/A

EXPERIMENTAL MODEL AND STUDY PARTICIPANT DETAILS

Plant material and growth conditions

Arabidopsis thaliana accessions Col-0 and a β -estradiol (E2) inducible Super-ETI line (SETI_wt), were used as the wild-type controls in this study. The lipase-like mutants SETI *eds1-2* (SETI_eds1), SETI *pad4-1* (SETI_pad4), SETI *sag101-1* (SETI_sag101), and SETI *pad4-1 sag101-1* (SETI_ps) and helper NLR mutants, including SETI *adr1-1 adr1-L1 adr1-L2 nrg1a nrg1b* (SETI_helperless), SETI *nrg1a nrg1b* (SETI_nrg1s), and SETI *adr1-1 adr1-L1 adr1-L2* (SETI_adr1s) are generated by crossing all the previously reported mutants with SETI plants.^{12,14,40}

For square and round plate assay, seeds were processed by liquid sterilization (70% ethanol 5 min, bleach solution 5 min, 100% ethanol 5 min, washed three times with sterilized water, and soaked into 0.05% agarose in 4°C dark condition for one day). Seeds were sown on a 9 cm Petri dish or square Petri dish (120 mm × 120 mm), GM (Germination media) plate, or GM plate with 50 μ M of E2. For square plates 1.2% agarose was used while for circular plates 0.8% agarose was used. Plants were grown at 21°C under long-day conditions (16 h light, 8 h dark), and at 50% humidity. Photos were taken 14 and 18 days after sowing. Col-0 was used as the negative and SETI as the positive control.

Bacterial strains and growth conditions

The various bacteria strains used in this study were described in the Key Resources Table. *Pseudomonas syringae* pv. tomato (*Pst*) DC3000 EV (carrying empty vector) grown on the King's B medium plates containing 25 μ g ml⁻¹ rifampicin, and 50 μ g ml⁻¹ kanamycin and *Pst* DC3000 hrc⁻ were grown on the King's B medium plates containing 25 μ g ml⁻¹ rifampicin. *Pseudomonas fluorescens* engineered with a Type III secretion system (Pf0-1 'EtHAN' strains) expressing empty vector was grown on the King's B medium plates with 50 μ g ml⁻¹ kanamycin, 34 μ g ml⁻¹ Chloramphenicol and 5 μ g ml⁻¹ tetracycline. All the *Pseudomonas* strains were grown on plates at 28°C for 2 days for further inoculum preparation.

METHOD DETAILS

Fresh weight measurement

The seeds were processed by liquid sterilization and sown on a square Petri dish, GM plate, or GM plate with 50 μ M of E2 for 18 days. Six seedlings were pooled together to measure the fresh weight. All statistics and figures are generated in R version 4.3.1. ANOVA ($p \leq 0.05$) was used for identifying significant factors. A least significant difference (LSD) test ($p \leq 0.05$) was used to identify differences between treatment and lines. A detailed statistical summary is available on GitHub: https://github.com/dinglab-plants/ETI_Project.

RNA-seq raw data processing, alignment, quantification of expression, and data visualization

DMSO in 10 mM MgCl₂, 50 μM E2 in 10 mM MgCl₂, *Pseudomonas fluorescens* (Pf0-1)⁴⁶ in 10 mM MgCl₂, or Pf0 and 50 μM E2 in 10 mM MgCl₂ was infiltrated in 5 to 6-week-old Arabidopsis leaves with 1 mL needleless syringe for RNA-seq sample collection. Two leaves per sample were collected at 0 and 4 hpi as 1 biological replicate. RNA was extracted with the Zymo RNA extraction kit.⁶²

The RNA sample was sequenced by Novogene. Raw reads were trimmed into 390 bp clean reads by the Novogene bioinformatics service. At least 12 million paired-end clean reads for each sample were provided by Novogene for RNA-seq analysis. All reads passed FastQC before the following analyses.⁶³ All clean reads were mapped either to the TAIR10 Arabidopsis genome/transcriptome via TopHat2 or to a comprehensive Reference Transcript Dataset for Arabidopsis Quantification of Alternatively Spliced Isoforms (AtRTD2_QUASI) containing 82,190 non-redundant transcripts from 34,212 genes via Galaxy and Salmon tools.^{64,65} The estimated gene transcript counts were used for differential gene expression analysis and statistical analysis with the 3D RNA-seq software.⁶¹ The low-expressed transcripts were filtered if they did not meet the criteria of ≥3 samples with ≥1 count per million reads. The batch effects between three biological replicates were removed to reduce artificial variance with the RUVSeq method.⁶⁶ The expression data were normalised across samples with the TMM (weighted trimmed mean of M-values).⁶⁷ The significance of expression changes in the contrasting groups 'SETI_wt_ETI vs. SETI_wt_mock', groups 'SETI_eds1_ETI vs. SETI_eds1_mock', 'SETI_pad4_ETI vs. SETI_pad4_mock', 'SETI_sag101_ETI vs. SETI_sag101_mock' and 'SETI_ps_ETI vs. SETI_ps_mock' were determined by the limma-voom method.^{68,69} A gene was defined as a significant differentially expressed gene (DEG) if it had a Benjamini-Hochberg adjusted P-value <0.01 and log₂[fold change (FC)] ≥ 1 (upregulated) or log₂[fold change (FC)] ≤ -1 (downregulated). The GO term analysis was analyzed with g:Profiler.⁶⁰

Electrolyte leakage assay

Two leaves of 5-week-old Arabidopsis plants were hand infiltrated using a 1-mL needleless syringe with 50 μM E2 dissolved in Milli-Q water or DMSO in Milli-Q water as mock. Leaf discs were collected with a 7-mm diameter cork borer from infiltrated leaves on paper towels. Leaf discs were dried and transferred into 2 mL of deionised water in 12-well plates (2 leaf disks per well). The plate was incubated for 30 min in a growth chamber with controlled conditions at 21°C under long-day conditions (16-h light/8-h dark) with a light intensity of 120–150 μmol m⁻². The water was replaced after incubation with 2 mL of deionised water. Electrolyte leakage was measured with Pocket Water Quality Meters (LAQUAtwin-EC-33; Horiba) calibrated at 1.41 mS/cm. Around 100 μL of the sample was used to measure conductivity at the indicated time points. ANOVA ($p \leq 0.05$) was used for identifying significant factors. Tukey-HSD-Test ($p \leq 0.05$) was used to determine differences between treatment and lines. A detailed statistical summary is available on GitHub: https://github.com/dinglab-plants/ETI_Project.

Semi-quantitative real-time PCR

Complementary DNAs (cDNAs) were synthesised from the RNA extracted for RNA-seq from SETI_wt and all lipase mutants in SETI background using a first-strand cDNA synthesis kit (Thermo Scientific) according to the manufacturer's instructions. 1 μL of cDNA was combined in a 15 μL reaction with 3mM dNTP, 2μM of each primer, 10xPCR buffer and Milli-Q water. Semi-quantitative real-time PCR (RT-PCR) analysis was performed using *AvrRps4* specific primers (*AvrRps4_F*: 5'-TCCAGCTTCAGTTACTCGGC-3'; *AvrRps4_R*: 5'-TTGGCTATTTTCGGCTGGGTT-3'). The elongation factor 1α (*EF1α*) primers (*EF1α_F*: 5'-CAGGCTGATTGTGCTGTTCTTA-3'; *EF1α_R*: 5'GTTGTATCCGACCTTCTTCAGG-3') were used as an internal control. The semi-quantitative RT-PCR reaction was performed as follows: pre-denaturation at 94°C (2 min), then 35 cycles at 94°C (15 s); 55°C (30 s) and 68°C (1 min), and a final extension at 68°C for (5 min). The RT-PCR products were electrophoresed and compared on 1.5% TAE agarose gel.

Bacterial growth assay

Pst DC3000 EV (carrying empty vector)⁴⁸ was grown on selective King's B (KB) medium plates containing 15% (w/v) agar, 25 μg ml⁻¹ rifampicin, and 50 μg ml⁻¹ kanamycin for 48 h at 28°C. Bacteria were harvested and resuspended in 10 mM MgCl₂. The concentration of the suspension was adjusted to an optical density of 0.001 at 600 nm [OD₆₀₀ = 0.001, representing ~5×10⁵ colony-forming units (CFU) ml⁻¹]. Two 5-week-old Arabidopsis leaves were hand infiltrated with 50 μM E2 dissolved in 10 mM MgCl₂ or DMSO in 10 mM MgCl₂ with a needleless syringe. The following day, the same leaves were infiltrated with bacteria. For quantification, leaf samples were harvested with a 7-mm diameter cork borer, resulting in leaf discs with an area of 0.38 cm². Two leaf discs per leaf were collected as a single sample. For each genotype and condition, four samples were collected immediately after infiltration as 'day 0' samples, and eight samples were collected at 3 dpi as 'day 3' samples to compare the bacterial titers between different genotypes, conditions, and treatments. For 'day 0', samples were ground in 200 μL of 10 mM MgCl₂ and spotted (10 μL per spot) on selective KB medium agar plates to grow for 48 h at 28°C. For 'day 3', samples were ground in 200 μL of infiltration buffer, serially diluted (5, 50, 5×10², 5×10³, 5×10⁴, 5×10⁵ times), and spotted (6 μL per spot) on selective King's B medium agar plates to grow for 48 h at 28°C. The number of colonies (CFU per drop) was counted, and bacterial growth was represented as CFU cm⁻² of leaf tissue. ANOVA ($p \leq 0.05$) was used for identifying significant factors. Tukey-HSD-Test ($p \leq 0.05$) was used to identify differences between treatment and lines. A detailed statistical summary is available on GitHub: https://github.com/dinglab-plants/ETI_Project.

Chlorophyll content estimation

Two leaves of 5-week-old *Arabidopsis* plants (SETI_wt, SETI_eds1, SETI_pad4, SETI_sag101, SETI_ps, SETI_adr1s, SETI_nrg1s, and SETI_helperless) were hand infiltrated using a 1 mL needleless syringe with 50 μ M E2 dissolved in 10 mM MgCl₂ as ETI treatment, *Pst* DC3000 *hrcC*⁻ (0.2 OD)⁴⁷ dissolved in 10 mM MgCl₂ as PTI treatment, E2+*Pst* DC3000 *hrcC*⁻ with same concentration as 'PTI+ETI' treatment and DMSO dissolved in 10 mM MgCl₂ as mock. Leaf disks were collected using a 7-mm diameter cork borer from 3 individual plants as 1 sample for each treatment. Samples were ground and resuspended in 1 mL of 80% acetone. The samples were then centrifuged at 10,000 g for 5 min. The absorbance of the supernatant was measured at 645 nm and 633 nm using UV-VIS spectrophotometer (UV-6300PC, VWR). Total and chlorophyll a, b content were calculated according to the following equations⁷⁰:

$$\text{Chl-a} = 12.72A_{663} - 2.59A_{645} / 1000 \text{ mg per g FW (mg g}^{-1}\text{)}$$

$$\text{Chl-b} = 22.9A_{645} - 4.67A_{663} / 1000 \text{ mg per g FW (mg g}^{-1}\text{)}$$

$$\text{Chl-t} = 20.31 A_{645} + 8.05 A_{663} / 1000 \text{ mg per g FW (mg g}^{-1}\text{)}$$

ANOVA ($p \leq 0.05$) was used for identifying significant factors. Tukey-HSD-Test ($p \leq 0.05$) was used to identify differences between treatment and lines. A detailed statistical summary is available on GitHub: https://github.com/dinglab-plants/ETI_Project.

QUANTIFICATION AND STATISTICAL ANALYSIS

R version 4.3.1 was used for data analysis. Boxplots and bar plots were generated using ggplot2. The heatmap on the right side in Figure 4 was generated with the R package 'ComplexHeatmap'.⁷¹ The UpSet plot and the volcano plot were generated with the R packages 'ComplexUpset'⁵¹ and 'EnhancedVolcano'.⁵² Figure S6 was done with 'gt'⁵³ and 'gtExtras'.⁵⁴ The following packages were used for data formatting and statistics: 'Tidyverse',⁴⁹ 'multcompView',⁵⁶ 'agricolae',⁵⁷ 'ggpubr',⁵⁸ 'stringr',⁵⁵ 'r2r',⁵⁹ and 'circlize'.⁵⁰ RNA-seq analysis was done as described above.